Widespread Increase of Tree Mortality Rates in the Western United States

Phillip J. van Mantgem, *et al.*

Science **323**, 521 (2009);
DOI: 10.1126/science.1165000

Science (print ISSN 0036-8075; online ISSN 1095-9203) is published weekly, except the last week in December, by the American Association for the Advancement of Science, 1200 New York Avenue NW, Washington, DC 20005.

the force generated by assembly of trans-SNARE complexes onto the two fusing membranes (Fig. 4), consistent with biochemical data (*23*). We postulate that after complexin binds to assembling SNARE complexes, its N-terminal sequence activates and clamps the force generated by SNARE-complex assembly. The N terminus of complexin might perform its activator function by pulling the complex closer to the membrane, possibly by binding to phospholipids, whereas the accessory N-terminal α-helix might clamp the complex by inserting into the space between the v- and t-SNAREs or even substituting for one of the SNAREs in the C-terminal segment of the trans-SNARE complex (*24*). Once anchored on the SNARE complex, the 40 N-terminal residues of complexin both activate and clamp SNARE complexes to control fast Ca^{2+}-triggered neurotransmitter release in a process that is conserved in all animals. Viewed in the broader picture, complexin and synaptotagmin therefore operate as interdependent clamp-activators of SNARE-dependent fusion, with synaptotagmin exploiting the activator effect of complexin and reversing its clamping function (*11*, *21*, *22*). In this molecular pas-de-deux, the functions of both proteins are intimately linked: Their phenotypes are identical both as activators and as clamps, and one does not operate without the other.

References and Notes

1. J. B. Sørensen, *Trends Neurosci.* **28**, 453 (2005).
2. R. Jahn, R. H. Scheller, *Nat. Rev. Mol. Cell Biol.* **7**, 631 (2006).
3. M. Verhage, R. F. Toonen, *Curr. Opin. Cell Biol.* **19**, 402 (2007).
4. M. Geppert *et al.*, *Cell* **79**, 717 (1994).
5. R. Fernandez-Chacon *et al.*, *Nature* **410**, 41 (2001).
6. M. Yoshihara, J. T. Littleton, *Neuron* **36**, 897 (2002).
7. K. Reim *et al.*, *Cell* **104**, 71 (2001).
8. X. Chen *et al.*, *Neuron* **33**, 397 (2002).
9. A. Bracher, J. Kadlec, H. Betz, W. Weissenhorn, *J. Biol. Chem.* **277**, 26517 (2002).
10. M. Xue *et al.*, *Nat. Struct. Mol. Biol.* **14**, 949 (2007).
11. C. G. Giraudo, W. S. Eng, T. J. Melia, J. E. Rothman, *Science* **313**, 676 (2006), published online 22 June 2006; 10.1126/science.1129450.
12. C. G. Giraudo *et al.*, *J. Biol. Chem.* **283**, 21211 (2008).
13. J. R. Schaub, X. Lu, B. Doneske, Y. K. Shin, J. A. McNew, *Nat. Struct. Mol. Biol.* **13**, 748 (2006).
14. T. Y. Yoon *et al.*, *Nat. Struct. Mol. Biol.* **15**, 707 (2008).
15. S. Huntwork, J. T. Littleton, *Nat. Neurosci.* **10**, 1235 (2007).
16. K. Weninger, M. E. Bowen, U. B. Choi, S. Chu, A. T. Brunger, *Structure* **16**, 308 (2008).
17. R. Guan, H. Dai, J. Rizo, *Biochemistry* **47**, 1474 (2008).
18. S. Schoch *et al.*, *Science* **294**, 1117 (2001).
19. Single-letter abbreviations for the amino acid residues are as follows: A, Ala; C, Cys; D, Asp; E, Glu; F, Phe; G, Gly; H, His; I, Ile; K, Lys; L, Leu; M, Met; N, Asn; P, Pro; Q, Gln; R, Arg; S, Ser; T, Thr; V, Val; W, Trp; and Y, Tyr.
20. For a description of the experimental procedures, see the supporting online material.
21. J. Tang *et al.*, *Cell* **126**, 1175 (2006).
22. A. Maximov, T. C. Südhof, *Neuron* **48**, 547 (2005).
23. K. Hu, J. Carroll, C. Rickman, B. Davletov, *J. Biol. Chem.* **277**, 41652 (2002).
24. C. G. Giraudo *et al.*, *Science* **323**, 512 (2009).

25. We thank J. Rizo and L. Chen for advice and critical comments. This study was supported by an investigatorship to T.C.S. from the Howard Hughes Medical Institute.

Supporting Online Material

www.sciencemag.org/cgi/content/full/323/5913/516/DC1
SOM Text
Figs. S1 to S14
Table S1
References

29 September 2008; accepted 5 December 2008
10.1126/science.1166505

Widespread Increase of Tree Mortality Rates in the Western United States

Phillip J. van Mantgem,[1]*†‡ Nathan L. Stephenson,[1]*† John C. Byrne,[2] Lori D. Daniels,[3] Jerry F. Franklin,[4] Peter Z. Fulé,[5] Mark E. Harmon,[6] Andrew J. Larson,[4] Jeremy M. Smith,[7] Alan H. Taylor,[8] Thomas T. Veblen[7]

Persistent changes in tree mortality rates can alter forest structure, composition, and ecosystem services such as carbon sequestration. Our analyses of longitudinal data from unmanaged old forests in the western United States showed that background (noncatastrophic) mortality rates have increased rapidly in recent decades, with doubling periods ranging from 17 to 29 years among regions. Increases were also pervasive across elevations, tree sizes, dominant genera, and past fire histories. Forest density and basal area declined slightly, which suggests that increasing mortality was not caused by endogenous increases in competition. Because mortality increased in small trees, the overall increase in mortality rates cannot be attributed solely to aging of large trees. Regional warming and consequent increases in water deficits are likely contributors to the increases in tree mortality rates.

As key regulators of global hydrologic and carbon cycles, forests are capable of contributing substantial feedbacks to global changes (*1*). Such feedbacks may already be under way; for example, forest carbon storage may be responding to environmentally driven changes in global patterns of tree growth and forest productivity (*2*–*4*). Recent warming has been implicated as contributing to episodes of forest dieback (pulses of greatly elevated tree mortality), such as those mediated by bark beetle outbreaks in western North America (*5*, *6*). Yet little effort has gone toward determining whether environmental changes are contributing to chronic, long-term changes in tree demographic rates (mortality and recruitment). Changes in demographic rates, when compounded over time, can alter forest structure, composition, and function (*7*). For example, a persistent doubling of background mortality rate (such as from 1 to 2% $year^{-1}$) ultimately would cause a >50% reduction in average tree age in a forest, and hence a potential reduction in average tree size. Additionally, changing demographic rates could indicate forests approaching thresholds for abrupt dieback. Yet spatially extensive analyses of long-term changes in tree demographic rates have been limited to tropical forests, where mortality and recruitment rates both have increased over the past several decades, perhaps in response to rising atmospheric CO_2 concentrations, nutrient deposition, or other environmental changes (*2*, *8*). Comparably extensive analyses have not been conducted in temperate forests.

We sought to determine whether systematic changes in tree demographic rates have occurred recently in coniferous forests of the western United States, and if so, to identify possible causes of those changes. Although the western United States has witnessed recent episodes of forest dieback related to bark beetle outbreaks or combinations of drought and outbreaks (*5*, *6*), most forested land continues to support seemingly healthy forests that have not died back (*9*). To minimize transient dynamics associated with stand development and succession, we limited our analyses to data from repeated censuses in undisturbed forest stands more than 200 years old (*10*). Old forests contain trees of all ages and sizes (*11*, *12*), and any large, persistent changes in demographic rates over a short period (such as a few decades) are likely to be consequences of exogenous environmental changes (*2*, *13*). In contrast, in young forests rapid demographic changes can sometimes result largely from endogenous processes (such as self-thinning during stand development) (*14*), potentially obscuring environmentally driven changes.

[1]U.S. Geological Survey, Western Ecological Research Center, Three Rivers, CA 93271, USA. [2]USDA Forest Service, Rocky Mountain Research Station, Moscow, ID 83843, USA. [3]Department of Geography, University of British Columbia, Vancouver, British Columbia V6T IZ2, Canada. [4]College of Forest Resources, University of Washington, Seattle, WA 98195, USA. [5]School of Forestry and Ecological Restoration Institute, Northern Arizona University, Flagstaff, AZ 86011, USA. [6]Department of Forest Science, Oregon State University, Corvallis, OR 97331, USA. [7]Department of Geography, University of Colorado, Boulder, CO 80309, USA. [8]Department of Geography, Pennsylvania State University, University Park, PA 16802, USA.

*These authors contributed equally to this work.
†To whom correspondence should be addressed. E-mail: pvanmantgem@usgs.gov (P.J.V.); nstephenson@usgs.gov (N.L.S.)
‡Present address: U.S. Geological Survey, Western Ecological Research Center, Arcata, CA 95521, USA.

Seventy-six long-term forest plots from three broad regions, spanning 14° of latitude and 18° of longitude and at elevations of 130 to 3353 m (Fig. 1 and table S1), met our criteria for analysis (*10*). Plots ranged from 0.25 to 15.75 ha ($\bar{x}$ = 1.33 ha), collectively containing 58,736 living trees over the study period, of which 11,095 died. The plots were originally established for diverse purposes—such as to investigate different stages of forest development, document dynamics of certain forest types, explore forest dynamics along environmental gradients, or act as controls for silvicultural experiments [see references in (*10*)]—that are unlikely to produce bias relative to our study's goals. We analyzed data from 1955 and later; only five plots from one region had earlier censuses. For individual plots, the initial census year analyzed ranged from 1955 to 1994 ($\bar{x}$ = 1981); the final census year ranged from 1998 to 2007 ($\bar{x}$ = 2004). Plots were censused three to seven times ($\bar{x}$ = 4.8). Our generally conservative estimates of forest ages at the time of initial censuses averaged ~450 years, with some plots exceeding 1000 years.

We used generalized nonlinear models to regress demographic rates on year; generalized nonlinear mixed models (GNMMs) were used when several plots were analyzed collectively (*10*). Demographic rates were estimated by annual compounding over the census interval length. All parameters were estimated by maximum likelihood.

Our models showed that mortality rates increased in 87% of plots (Fig. 1) ($P < 0.0001$, two-tailed binomial test). Mortality rate increased significantly for all plots combined and in each of the three regions (Fig. 2 and Table 1), with estimated doubling periods ranging from 17 years (Pacific Northwest) to 29 years (interior). Mortality rates also increased at low, middle, and high elevations (<1000 m, 1000 to 2000 m, and >2000 m, respectively) and for small, medium, and large trees (stem diameter <15 cm, 15 to 40 cm, and >40 cm, respectively) (Fig. 2 and Table 1). The three most abundant tree genera in our plots (comprising 77% of trees) are dominated by different life history traits (*Tsuga*, late successional; *Pinus*, generally shade-intolerant; *Abies*, generally shade-tolerant); all three showed increasing mortality rates (Fig. 2 and Table 1). An introduced fungal pathogen, *Cronartium ribicola*, is known to contribute to increasing mortality rates in five-needled species of *Pinus* (*15*). When all five-needled *Pinus* were removed from analysis, mortality rates among the remaining *Pinus* (those immune to the pathogen) still increased [$a = 0.027$, $P = 0.0011$, GNMM, $n = 22$, where a is the estimated annual fractional change in mortality rate; see (*10*)]. Finally, trees belonging to the remaining 16 genera (23% of all trees) collectively showed increasing mortality rates (Fig. 2 and Table 1).

In contrast to mortality rates, recruitment rates increased in only 52% of plots—a proportion indistinguishable from random ($P = 0.80$, two-tailed binomial test). There was no detectable trend in recruitment for all plots combined, nor when regions were analyzed separately ($P \geq 0.20$, GNMM; table S2).

We examined three classes of possible causes of the increasing tree mortality rates: methodological artifacts, endogenous processes, and exogenous processes. We tested for and ruled out several obvious potential sources of methodological artifacts (*10*). Among endogenous processes, perhaps the best-known cause of increasing tree mortality rates is increasing competition resulting from increasing forest density and basal area (*11*, *12*). Such changes might especially be expected in the subset of old forests in the western United States that formerly experienced frequent surface fires; in these forests, fire exclusion (generally spanning the last century) often resulted in an initial increase in forest density and basal area (*16*, *17*). However, consistent with our observations of increasing mortality without compensating increases in recruitment, forest density and basal area declined slightly during the study period

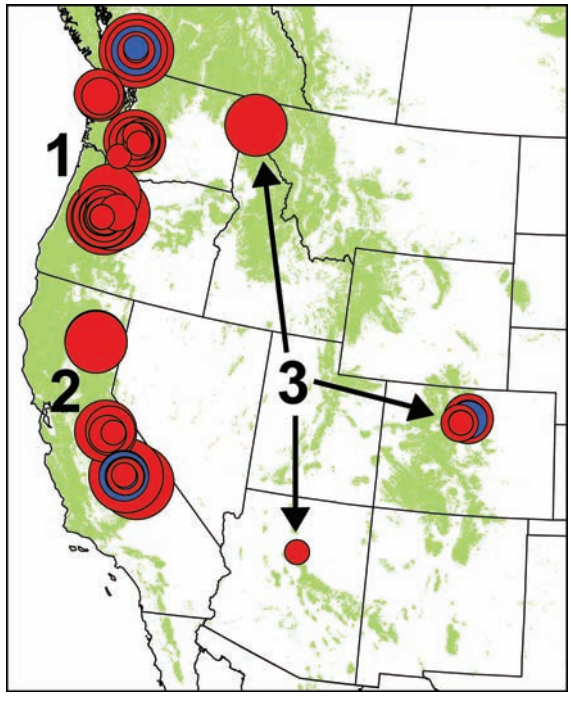

Fig. 1. Locations of the 76 forest plots in the western United States and southwestern British Columbia. Red and blue symbols indicate, respectively, plots with increasing or decreasing mortality rates. Symbol size corresponds to annual fractional change in mortality rate (smallest symbol, <0.025 year^{-1}; largest symbol, >0.100 year^{-1}; the three intermediate symbol sizes are scaled in increments of 0.025 year^{-1}). Numerals indicate groups of plots used in analyses by region: (1) Pacific Northwest, (2) California, and (3) interior. Forest cover is shown in green.

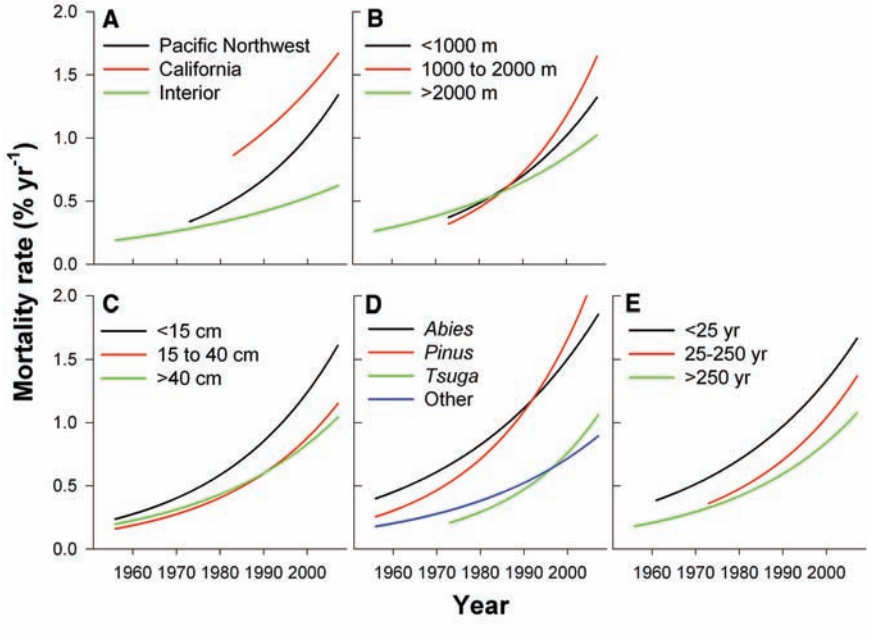

Fig. 2. Modeled trends in tree mortality rates for (**A**) regions, (**B**) elevational class, (**C**) stem diameter class, (**D**) genus, and (**E**) historical fire return interval class.

[$P \leq 0.028$, linear mixed model (LMM); fig. S1]. Thus, forest structural changes are consistent with a slight decline rather than an increase in potential for competition over the study period, which suggests that increasing mortality rates cannot be attributed to changes in forest structure.

Fire exclusion conceivably could affect mortality rates through mechanisms unrelated to forest structural changes, such as allowing increases in insects or pathogens that were formerly controlled by fire. We therefore classified plots by their pre–fire exclusion fire return intervals: short, intermediate, and long (<25 years, 25 to 250 years, and >250 years, respectively) (table S1). If fire exclusion ultimately were responsible for increasing tree mortality rates, we would expect to see increases in plots with historically short fire return intervals (which have experienced substantial recent changes in fire regime) and little or no change in mortality rates in plots with historically long return intervals (which have experienced little or no change in fire regime). However, mortality rates showed comparable increases in each of the three classes (Fig. 2 and Table 1); we therefore conclude that fire exclusion is an unlikely cause of the observed increases in mortality rates.

Mortality rates could increase if a cohort of old trees begins to die and fall, crushing smaller trees at an increasing rate [a mechanism related to the proposed "majestic forest" effect; see references in (*8*)]. If such a mechanism were responsible for the observed increase in tree mortality rates, we would expect to see no parallel increase in mortality rates of small trees that died standing (i.e., trees <15 cm in diameter that died of causes other than being crushed by falling trees from an aging cohort), because such deaths are independent of deaths in an aging cohort. However, the mortality rate of small trees that died standing increased rapidly in recent decades, doubling in ~16 years ($P < 0.0001$, GNMM; table S3); thus, other mechanisms must be acting. Finally, mortality rates increased in all major genera rather than being limited to those dominated by a particular life history trait (such as shade intolerance), which suggests that successional dynamics are unlikely to be primary drivers of increasing mortality rates.

We conclude that endogenous processes are unlikely to be major contributors to the observed rapid, synchronous doubling of mortality rates in our heterogeneous sample of old forests at a subcontinental scale. Moreover, the available evidence is inconsistent with major roles for two possible exogenous causes: forest fragmentation and air pollution (*10*).

We suggest that regional warming may be the dominant contributor to the increases in tree mortality rates. From the 1970s to 2006 (the period including the bulk of our data; table S1), the mean annual temperature of the western United States increased at a rate of 0.3° to 0.4°C decade^{-1}, even approaching 0.5°C decade^{-1} at the higher elevations typically occupied by forests (*18*). This regional warming has contributed to widespread hydrologic changes, such as declining fraction of precipitation falling as snow (*19*), declining snowpack water content (*20*), earlier spring snowmelt and runoff (*21*), and a consequent lengthening of the summer drought (*22*). Specific to our study sites, mean annual precipitation showed no directional trend over the study period ($P = 0.62$, LMM), whereas both mean annual temperature and climatic water deficit (annual evaporative demand that exceeds available water) increased significantly ($P < 0.0001$, LMM) (*10*). Furthermore, temperature and water deficit were positively correlated with tree mortality rates ($P \leq 0.0066$, GNMM; table S4).

Warming could contribute to increasing mortality rates by (i) increasing water deficits and thus drought stress on trees, with possible direct and indirect contributions to tree mortality (*13*, *23*); (ii) enhancing the growth and reproduction of insects and pathogens that attack trees (*6*); or (iii) both. A contribution from warming is consistent with both the apparent role of warming in episodes of recent forest dieback in western North America (*5*, *6*) and the positive correlation between short-term fluctuations in background mortality rates and climatic water deficits observed in California and Colorado (*13*, *24*).

The rapid and pervasive increases in tree mortality rates in old forests of the western United States are notable for several reasons. First, increasing mortality rates could presage substantial changes in forest structure, composition, and function (*7*, *25*), and in some cases could be symptomatic of forests that are stressed and vulnerable to abrupt dieback (*5*). Indeed, since their most recent censuses, several of our plots in the interior region experienced greatly accelerated mortality due to bark beetle outbreaks, and in some cases nearly complete mortality of large trees (*10*). Second, the increasing mortality rates demonstrate that ongoing, subcontinental-scale changes in tree demographic rates are not limited to the tropics (*8*). Third, some of the changes in the western United States contrast sharply with those in the tropics, where increasing mortality rates have been paralleled by increasing recruitment rates and basal area (*2*, *8*). In the western United States, recruitment rates have not changed while forest density and basal area have declined slightly. Fourth, our results are inconsistent with a major role for endogenous causes of increasing mortality rates. Instead, the evidence is consistent with contributions from exogenous causes, with regional warming and consequent drought stress being the most likely drivers.

Table 1. Fixed effects of generalized nonlinear mixed models describing mortality rate trends (*10*); *a* is the estimated annual fractional change in mortality rate (*10*) and *n* is the number of forest plots used in the model.

Model	Data	*a*	SE	*P*	*n*
Mortality trend	All plots	0.039	0.005	<0.0001	76
Mortality trend by region	Pacific Northwest	0.042	0.006	<0.0001	47
	California	0.028	0.009	0.0050	20
	Interior	0.024	0.009	0.0319	9
Mortality trend by elevation class	<1000 m	0.038	0.007	<0.0001	33
	1000 to 2000 m	0.050	0.010	<0.0001	20
	>2000 m	0.027	0.006	0.0003	23
Mortality trend by stem diameter class	<15 cm	0.039	0.006	<0.0001	61
	15 to 40 cm	0.040	0.006	<0.0001	76
	>40 cm	0.033	0.007	<0.0001	76
Mortality trend by genus	*Abies*	0.031	0.010	0.0025	62
	Pinus	0.044	0.010	<0.0001	37
	Tsuga	0.049	0.009	<0.0001	47
	All other genera	0.032	0.008	<0.0001	64
Mortality trend by fire return interval	<25 years	0.033	0.008	0.0009	15
	25 to 250 years	0.040	0.006	<0.0001	32
	>250 years	0.036	0.010	0.0008	29

References and Notes

1. G. B. Bonan, *Science* **320**, 1444 (2008).
2. S. L. Lewis *et al.*, *Philos. Trans. R. Soc. London Ser. B* **359**, 421 (2004).
3. A. S. Jump, J. M. Hunt, J. Peñuelas, *Glob. Change Biol.* **12**, 2163 (2006).
4. K. J. Feeley, S. J. Wright, M. N. Nur Supardi, A. R. Kassim, S. J. Davies, *Ecol. Lett.* **10**, 461 (2007).
5. D. D. Breshears *et al.*, *Proc. Natl. Acad. Sci. U.S.A.* **102**, 15144 (2005).
6. K. F. Raffa *et al.*, *Bioscience* **58**, 501 (2008).
7. R. K. Kobe, *Ecol. Monogr.* **66**, 181 (1996).
8. O. L. Phillips *et al.*, *Philos. Trans. R. Soc. London Ser. B* **359**, 381 (2004).
9. J. A. Hicke, J. C. Jenkins, D. S. Ojima, M. Ducey, *Ecol. Appl.* **17**, 2387 (2007).
10. See supporting material on *Science* Online.
11. C. D. Oliver, B. C. Larson, *Forest Stand Dynamics* (McGraw-Hill, New York, 1990).
12. J. F. Franklin *et al.*, *For. Ecol. Manage.* **155**, 399 (2002).
13. P. J. van Mantgem, N. L. Stephenson, *Ecol. Lett.* **10**, 909 (2007).
14. J. A. Lutz, C. B. Halpern, *Ecol. Monogr.* **76**, 257 (2006).
15. G. I. McDonald, R. J. Hoff, in *Whitebark Pine Communities*, D. F. Tomback, S. F. Arno, R. E. Keane, Eds. (Island Press, Washington, DC, 2001), pp. 193–220.
16. R. T. Brown, J. K. Agee, J. F. Franklin, *Conserv. Biol.* **18**, 903 (2004).
17. M. North, J. Innes, H. Zald, *Can. J. For. Res.* **37**, 331 (2007).
18. H. F. Diaz, J. K. Eischeid, *Geophys. Res. Lett.* **34**, L18707 (2007).

19. N. Knowles, M. D. Dettinger, D. R. Cayan, *J. Clim.* **19**, 4545 (2006).
20. P. W. Mote, A. F. Hamlet, M. P. Clark, D. P. Lettenmaier, *Bull. Am. Meteorol. Soc.* **86**, 39 (2005).
21. I. T. Stewart, D. R. Cayan, M. D. Dettinger, *J. Clim.* **18**, 1136 (2005).
22. A. L. Westerling, H. G. Hidalgo, D. R. Cayan, T. W. Swetnam, *Science* **313**, 940 (2006); published online 5 July 2006 (10.1126/science.1128834).
23. N. McDowell *et al.*, *New Phytol.* **178**, 719 (2008).
24. C. Bigler, D. G. Gavin, C. Gunning, T. T. Veblen, *Oikos* **116**, 1983 (2007).
25. A. W. Fellows, M. L. Goulden, *Geophys. Res. Lett.* **35**, L12404 (2008).

26. We thank the many people involved in establishing and maintaining the permanent forest plots; C. Allen, A. Das, J. Halofsky, J. Hicke, J. Lutz, and four anonymous reviewers for helpful comments on the manuscript; and J. Yee for essential statistical advice. The forest plots were funded by NSF's Long-term Studies Program (DEB-0218088); the Wind River Canopy Crane Program through cooperative agreement PNW 08-DG-11261952-488 with the USDA Forest Service Pacific Northwest Research Station; various awards through the USDA Forest Service's Pacific Northwest, Pacific Southwest, and Rocky Mountain research stations and the McIntire-Stennis Cooperative Forestry Program; NSF awards DEB-0743498 and BCS-0825823; the Natural Science and Engineering Research Council of Canada; and various awards through the U.S. National Park Service and U.S. Geological Survey (USGS). This work is a contribution of the Western Mountain Initiative (a USGS global change research project) and the Cordillera Forest Dynamics Network (CORFOR).

Supporting Online Material

www.sciencemag.org/cgi/content/full/323/5913/521/DC1
Materials and Methods
SOM Text
Figs. S1 to S6
Tables S1 to S4
References

22 August 2008; accepted 3 December 2008
10.1126/science.1165000

The Sphingolipid Transporter Spns2 Functions in Migration of Zebrafish Myocardial Precursors

Atsuo Kawahara,[1,2]* Tsuyoshi Nishi,[3,4] Yu Hisano,[3,4] Hajime Fukui,[1] Akihito Yamaguchi,[3,4] Naoki Mochizuki[1]

Sphingosine-1-phosphate (S1P) is a secreted lipid mediator that functions in vascular development; however, it remains unclear how S1P secretion is regulated during embryogenesis. We identified a zebrafish mutant, *ko157*, that displays cardia bifida (two hearts) resembling that in the *S1P receptor-2* mutant. A migration defect of myocardial precursors in the *ko157* mutant is due to a mutation in a multipass transmembrane protein, Spns2, and can be rescued by S1P injection. We show that the export of S1P from cells requires Spns2. *spns2* is expressed in the extraembryonic tissue yolk syncytial layer (YSL), and the introduction of *spns2* mRNA in the YSL restored the cardiac defect in the *ko157* mutant. Thus, Spns2 in the YSL functions as a S1P transporter in S1P secretion, thereby regulating myocardial precursor migration.

During the late stages of zebrafish segmentation characterized by the formation of the somites, the myocardial precursors from both sides of the anterior lateral plate mesoderm migrate toward the midline to form the heart tube (*1*, *2*). Forward genetic analysis in zebrafish has helped to uncover genes involved in vertebrate heart formation (*3*). To identify additional regulators of heart development, we performed *N*-ethyl-*N*-nitrosourea (ENU) mutagenesis screening for mutations specifically affecting cardiac morphogenesis. We isolated a recessive *ko157* mutant that displayed two hearts, a condition known as cardia bifida with swollen pericardial sacs (Fig. 1, A, B, E, and F). The expression of myocardial markers [*nkx2.5* and *cardiac myosin light chain 2* (*cmlc2*)] and chamber-specific markers [*atrial myosin heavy chain* (*amhc*) and *ventricular myosin heavy chain* (*vmhc*)] was detected in two separated domains (Fig. 1, C and G, and fig. S2); this finding suggests that the myocardial precursors failed to migrate but differentiated into two chambers at the bilateral positions.

The migration of several mesodermal derivatives examined by the expression pattern of a vascular marker (*fli1*), an erythroid marker (*gata1*), a pronephric marker (*pax2*), and a lateral plate mesoderm marker (*hand2*) was not impaired in *ko157* mutants (figs. S2 and S3), which suggests that the migration of myocardial precursors is dominantly affected. Besides cardia bifida, there were abnormal blisters at the tip of the tail in the mutant (Fig. 1, D and H). These two characteristic phenotypes (cardia bifida and tail blisters) in the *ko157* mutant were similar to those in the *miles apart* (*mil*)/*S1P receptor-2* (*S1P2*) mutant (*4*). Sphingosine-1-phosphate (S1P) is a lipid mediator involved in cell growth, death, migration, and differentiation (*5*–*8*). Both cardia bifida and tail blisters were observed in embryos injected with an antisense morpholino for *mil/S1P2* (*mil* MO; 15 ng) (*9*) (fig. S4 and table S1), suggesting a genetic interaction between *ko157* and *mil/S1P2*.

Genetic mapping of the *ko157* mutation by means of simple sequence length polymorphism

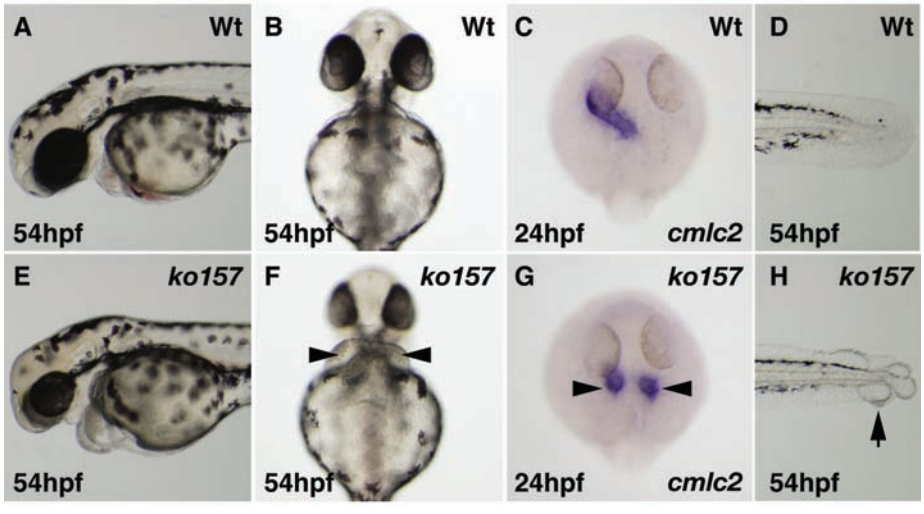

Fig. 1. Morphological phenotypes of *ko157* mutants. (**A**, **B**, **D**, **E**, **F**, and **H**) Stereomicroscopic views of wild-type (Wt) embryo [(A), (B), and (D)] and *ko157* mutant [(E), (F), and (H)]. Two swollen pericardial sacs (arrowheads) at 54 hours post-fertilization (hpf) were observed in *ko157* mutant [(E) and (F)] but not in Wt embryos [(A) and (B)]. (B) and (F) are ventral views. (**C** and **G**) Two hearts (arrowheads) in *ko157* mutants at 24 hpf were visualized (dorsal view) by whole-mount in situ hybridization with antisense *cmlc2* probe. *ko157* mutant (H), but not Wt embryos (D), exhibited tail blisters (arrow).

[1]Department of Structural Analysis, National Cardiovascular Center Research Institute, Fujishirodai 5-7-1, Suita, Osaka 565-8565, Japan. [2]HMRO, Kyoto University Faculty of Medicine, Yoshida, Sakyo-Ku, Kyoto 606-8501, Japan. [3]Department of Cell Membrane Biology, Institute of Scientific and Industrial Research, Osaka University, 8-1 Mihogaoka, Ibaraki-shi, Osaka 567-0047, Japan. [4]Graduate School of Pharmaceutical Sciences, Osaka University, Suita-shi, Osaka 565-0871, Japan.

*To whom correspondence should be addressed. E-mail: atsuo@ri.ncvc.go.jp

www.sciencemag.org/cgi/content/full/323/5913/521/DC1

Supporting Online Material for

Widespread Increase of Tree Mortality Rates in the Western United States

Phillip J. van Mantgem,* Nathan L. Stephenson,* John C. Byrne, Lori D. Daniels, Jerry F. Franklin, Peter Z. Fulé, Mark E. Harmon, Andrew J. Larson, Jeremy M. Smith, Alan H. Taylor, Thomas T. Veblen

*To whom correspondence should be addressed. E-mail: pvanmantgem@usgs.gov (P.J.V.); nstephenson@usgs.gov (N.L.S.)

Published 23 January 2009, *Science* **323**, 521 (2009)
DOI: 10.1126/science.1165000

This PDF file includes:

SUPPORTING ONLINE MATERIAL

Widespread Increase of Tree Mortality Rates in the Western United States

P.J. van Mantgem, N.L. Stephenson, J.C. Byrne, L.D. Daniels, J.F. Franklin, P.Z. Fulé, M.E. Harmon, A.J. Larson, J.M. Smith, A.H. Taylor, T.T. Veblen

Supporting Materials and Methods

Data

For reasons given below, we limited analyses to forest plots meeting the following eight criteria. (*i*) Analyses were limited to plots in which the fates of individual trees were tracked through repeated censuses. This conservative approach allowed us to avoid possible problems associated with retrospective analyses. For example, dendrochronological (tree-ring) approaches to estimating demographic rates can suffer imprecision in estimated year of tree death (*S1*) and a "fading record" problem (the disproportionate loss of records from trees that have been dead the longest) (*S2*). (*ii*) To minimize transient dynamics associated with stand development and succession (*S3, S4*), we assessed only forests in which the last stand-replacing disturbance occurred >200 years ago, as estimated by counting rings on increment cores or nearby stumps, or by local historical records and the sizes of the largest trees. (*iii*) Because we also wished to minimize transient dynamics associated with less severe but more recent disturbances, we used only plots with no evidence of fire, flood, avalanche, or tree cutting in the last several decades. (*iv*) To ensure our samples of tree populations were complete and unbiased, we used plots in which every tree above a defined diameter at breast height (dbh, 1.4 m above ground level) was sampled at the initial census used in our analyses (Table S1). We made an exception for four plots in which tree recruitment had been measured inconsistently (FRB2, FRC3, FRD2, FRD1; Table S1); at the first censuses used in analyses, data from these four plots did not include small trees that had recruited in the preceding 13 to 22 years. (*v*) Because individual plots are our unit of analysis, we limited analyses to plots large enough and containing enough trees to reduce random variation in plot-level demographic rates (*S5*). We therefore required that plots were ≥0.25 ha and contained >100 trees at their first census. (*vi*) All plots had at least three complete censuses, a requirement for comparing demographic rates from at least two different time intervals. (*vii*) We limited analyses to plots with records of sufficient length to detect possible long-term demographic changes – those with ≥10 years of record between their first and last censuses. (*viii*) Finally, both because the vast majority of available data was from recent decades and because we were most interested in exploring recent demographic changes, we required that final censuses for all plots occurred within the last 10 years (1998 or later).

To find data meeting these criteria, we began by examining an extensive literature review and data compilation (*S6*). We sought additional data sources by contacting colleagues at universities and long-term forest research sites, such as those in the USDA Forest Service's Experimental Forest and Research Natural Area networks, the U.S. National Science Foundation's Long-Term Ecological Research network, and the U.S. National Park Service's Inventory and Monitoring network. Most forest plots did not meet our criteria, usually because

they lacked three or more complete censuses or were not in undisturbed old forest. Data requirements precluded some extensive and well-known plot networks, such as the USDA Forest Service's Forest Inventory and Analysis network (*S7*), which in the western United States lacked three complete censuses in which the fates of individual trees were tracked. Plots and plot networks meeting our criteria (Table S1) are described in more detail elsewhere (*S8-14*). Subsequent to their most recent censuses, some of our plots in the interior region experienced greatly accelerated mortality due to bark beetle outbreaks (plots FRB2, FRC3, FRD1, and FRD2 in Colorado, last censused in 2004, and Gus Pearson in Arizona, last censused in 2000), and in some cases nearly complete mortality of large trees. Lacking subsequent censuses, these recent mortality episodes could not be included in our analyses.

Census intervals for the majority of qualifying plots averaged ~6 years. To increase consistency in interval lengths among regions, for the region with annual-resolution demographic data (California; Table S1) we analyzed data at ~5 year intervals; exact interval lengths were determined by the intervals between tree diameter remeasurements in these plots.

Newly-recruited trees (those that for the first time meet the minimum dbh threshold for a given plot) were added to populations at each census and were included in all subsequent analyses. Fifteen of our 76 plots lacked consistent recruitment data for all censuses, and were therefore precluded from analyses of recruitment trends (plots LDUN, LD1A, LD1B, LD1C, LDMA, LD2C, LD2B, MRS5, MRS7, BW2, FRB2, FRC3, FRD2, FRD1, and Gus Pearson; Table S1). All else being equal, mortality rate calculations for these 15 plots are expected to be biased toward yielding declining mortality rates through time (*S15*). When a group of trees is tracked without addition of new recruits at each census, subpopulations of trees with intrinsically high mortality rates [often the smallest trees (*S16*)] will, through time, decline in relative abundance compared to subpopulations with intrinsically low mortality rates, so that calculated mortality rates for the plot as a whole may decline with each subsequent census (*S15*). However, in spite of their potential bias toward declining mortality rates, these 15 plots showed significantly increasing mortality rates (a=0.025, S.E.=0.011, P=0.0363, generalized nonlinear mixed model).

To estimate climate associated with individual plots (most of which lie in complex mountainous terrain without adjacent weather stations), we used outputs from the Parameter-elevation Regression on Independent Slopes Model (PRISM) (*S17-18*). PRISM interpolates climate at a 4 km grid resolution from instrumental observations and a digital elevation model, making adjustments for features such as elevation, aspect, slope, and rainshadows. We used PRISM-derived monthly average temperature and precipitation with a modified Thornthwaite method (*S19*) to calculate annual climatic water deficit – a biologically meaningful index of unmet evaporative demand (drought) that is responsive to changes in both temperature and precipitation (*S20*). Climatic parameters were calculated for water years (October through September). For modeling with demographic data, we averaged annual climatic measurements across all years within each census interval for the associated plot.

Statistical Models

We sought statistical models that were simple, appropriate to the data, and capable of detecting directional changes in demographic rates. Plot-specific trends in demographic rates were analyzed with generalized nonlinear models. When analyzing trends across multiple plots, we added a normal random effect based on plot identity to the linear function to account for

differences among plots. Specifically, to estimate changes in annual mortality rates we modeled the rate as a logistic function $\exp(\beta_0 + \beta_1 t_j + \gamma_i)/\left(1+\exp(\beta_0 + \beta_1 t_j + \gamma_i)\right)$. We applied a statistical model to our data where n_{ij} was the number of trees alive at the previous census for the ith plot and the jth census, and m_{ij} the corresponding count of mortalities

$$m_{ij} \mid \gamma_i \sim \text{ Negative binomial with mean } n_{ij} p_{ij} \text{ and variance } n_{ij} p_{ij} \left(\frac{n_{ij} p_{ij} + \alpha^{-1}}{\alpha^{-1}} \right) \qquad (1)$$

$$p_{ij} = 1 - \left(1+\exp(\beta_0 + \beta_1 t_j + \gamma_i)\right)^{-c_j}, \qquad \gamma_i \sim N\left(0, \sigma_\gamma^2\right) \qquad (2)$$

where p_{ij} represents the probability of mortality over the census interval, t_j represents the year of the jth census, and c represents the census interval length in years. The random intercept parameter (γ_i) follows a normal distribution. The negative binomial distribution is an extension of the Poisson distribution with $\alpha>0$ representing overdispersion.

We modeled annual recruitment rates as $\exp(\beta_0 + \beta_1 t_j + \gamma_i)$ and applied a similar statistical model where r_{ij} is the count of recruits

$$r_{ij} \mid \gamma_i \sim \text{ Negative binomial with mean } n_{ij} p_{ij} \text{ and variance } n_{ij} p_{ij} \left(\frac{n_{ij} p_{ij} + \alpha^{-1}}{\alpha^{-1}} \right) \qquad (3)$$

$$p_{ij} = \left(1+\exp\left(\beta_0 + \beta_1 t_j + \gamma_i\right)\right)^{c_j} - 1, \qquad \gamma_i \sim N\left(0, \sigma_\gamma^2\right) \qquad (4)$$

where p_{ij} represents the rate of recruitment over the census interval.

We used maximum likelihood to estimate model parameters producing the most likely annual demographic rates that, when compounded by the length of the census intervals, best corresponded to the rates observed in the data. We tested models that included parameters for random slopes among plots and additional polynomial terms, but found little support for these models. Estimated annual fractional changes in mortality and recruitment rates (a) were calculated as $\exp(\beta_1)$-1, which provides an exact value for recruitment rates and, when mortality rates are small (as they are in this study), a close approximation of fractional changes for mortality rates.

Trends in forest density, basal area, climatic parameters, and census interval length were estimated using linear mixed models (LMM); for forest density and basal area we used only the 61 plots with recruitment data at each census. Substantial temporal autocorrelation was accounted for with a first order autoregressive autocorrelation function. Problems with heteroscedasticity, when present, were resolved by allowing different variance components among logical groups (e.g., plots with low vs. high forest density).

Assessing Possible Methodological Problems

Mantel tests showed no evidence of positive spatial autocorrelation among all plots considered together, or among plots within regions, for (*i*) average mortality rate ($P \geq 0.77$), (*ii*)

annual fractional change in mortality rate ($P \geq 0.68$), and (*iii*) residuals of the plot identity random effect ($P \geq 0.72$). The lack of spatial autocorrelation is not surprising; our plots primarily occur in heterogeneous mountainous terrain, where close geographic proximity does not imply similarity in forest characteristics or in climatic, edaphic, or topographic environments.

If census interval length declines through time, calculated mortality rate can increase even though the underlying rate has remained constant (*S15, S21*). However, the effect is slight (*S21*), and our plots collectively showed no trend in census interval lengths through time (β_{year}= -0.013, S.E.= 0.015, P=0.39, LMM, where β_{year} represents the slope of annual change). Increasing mortality rates were also unrelated to the addition of new plots through time; mortality rates increased for plots established on or before 1975, 1980, 1985, and 1990 (Table S3).

To explore whether heterogeneity in plot characteristics might affect a (modeled annual fractional changes in mortality rates), we regressed calculated values of a for individual plots on plot size, average census interval length, and forest density, all of which vary widely among plots. A single plot, CIRQUE (Table S1), was initially dropped from this analysis. CIRQUE was the only plot to record no mortalities during a census interval (the first of two intervals), leading to a modeled value of a that was orders of magnitude greater than that of other plots. (This lack of mortality during one interval was of no concern in the mixed models, in which all other plots recorded mortality in all intervals.) Our linear regressions showed that a was uncorrelated with plot size, average census interval length, and forest density (Fig. S2); all regressions remained non-significant when CIRQUE was added. We therefore conclude that even though plot size, average census interval length, and forest density vary widely among plots, they have no detectible effect on modeled annual fractional changes in mortality rates.

We used simple analyses and graphs as independent checks on model results for the three regions. Consistent with model results, graphed mortality rates of individual plots, though quite variable, collectively increased through time (Figs. S3-S5). Because potential biases associated with "site switching" prevented us from simply graphing averaged mortality rates by year (see *S22*), we instead compared mean mortality rates of first and last census intervals (Fig. S6). Consistent with model results, for each region mean mortality rate of the last census interval was significantly higher than that of the first interval (Pacific Northwest, P<0.0001; California, P<0.0001; interior, P=0.0078, paired permutation tests).

Supporting Text

Assessing Possible Exogenous Causes of Increasing Mortality Rates

We can reasonably reject increasing rates of forest fragmentation as a source of increasing tree mortality rates. In tropical Amazonia, trees up to 300 m from forest edges experience higher mortality rates due to windthrow and microclimatic changes (*S23*). However, 33 of our plots lie deep within national parks protected from logging. Mortality rate in these plots increased, at a rate comparable to plots outside of parks (Table S3).

While air pollution might enhance susceptibility of some of our study forests to other stresses, we consider it an unlikely cause of the widespread increase in mortality rates. Ozone – arguably the atmospheric pollutant most likely to affect tree survival in the western United States – varies greatly in concentration across the western United States (*S24*). Even the Pacific Northwest, the study region with ozone concentrations too low to be considered significant

influences on tree survival, showed strongly increasing mortality rates (see Fig. 2 and Table 1 in the main article). Additionally, in California (the study region with highest ozone concentrations), concentrations did not increase during the study period (*S24*), though mortality rates did. Further, short-term fluctuations in ozone concentrations were not correlated with tree mortality rates in California (*S11*).

Climatic data modeled for all plots indicated increasing average temperatures (β_{year}=0.026, S.E.= 0.002, P<0.0001, LMM) with no trend in precipitation (β_{year}=0.289, S.E.=0.577, P=0.616, LMM), together resulting in significant increases in climatic water deficits (β_{year}=1.101, S.E.= 0.114, P<0.0001, LMM). Both average temperature and climatic water deficit were positively correlated with tree mortality rates (Table S4). Even though the rather coarse resolution of demographic data used in our analyses (mean census interval length ~6 years) may have obscured correlations between short-term fluctuations in environmental conditions and demographic rates, previous annual-resolution analyses of our California data revealed a strong positive correlation between short-term fluctuations in water deficits and tree mortality rates (*S11*).

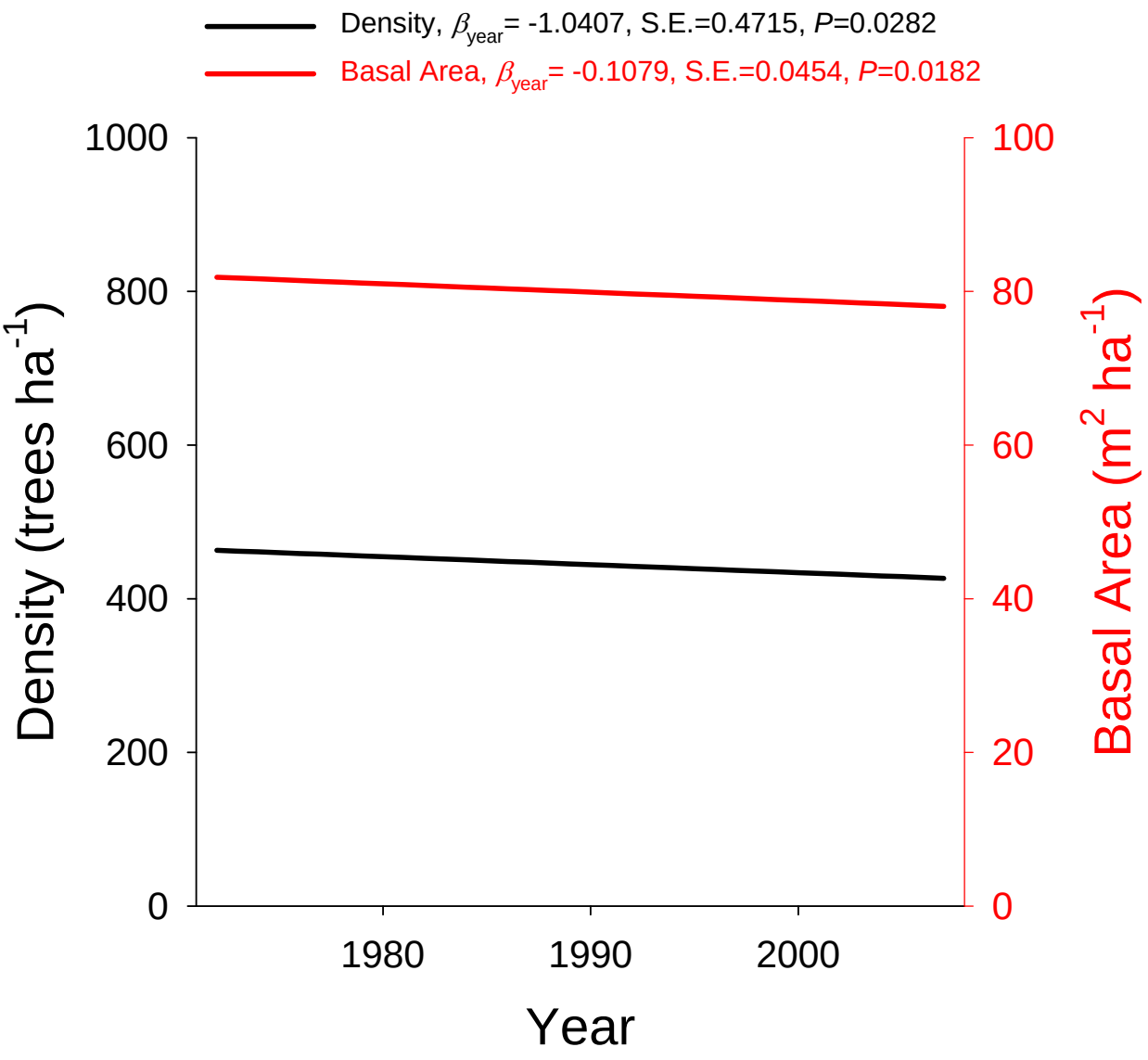

Figure S1. Trends in forest density (black line) and basal area (red line) from linear mixed models for the 61 forest plots with complete recruitment data.

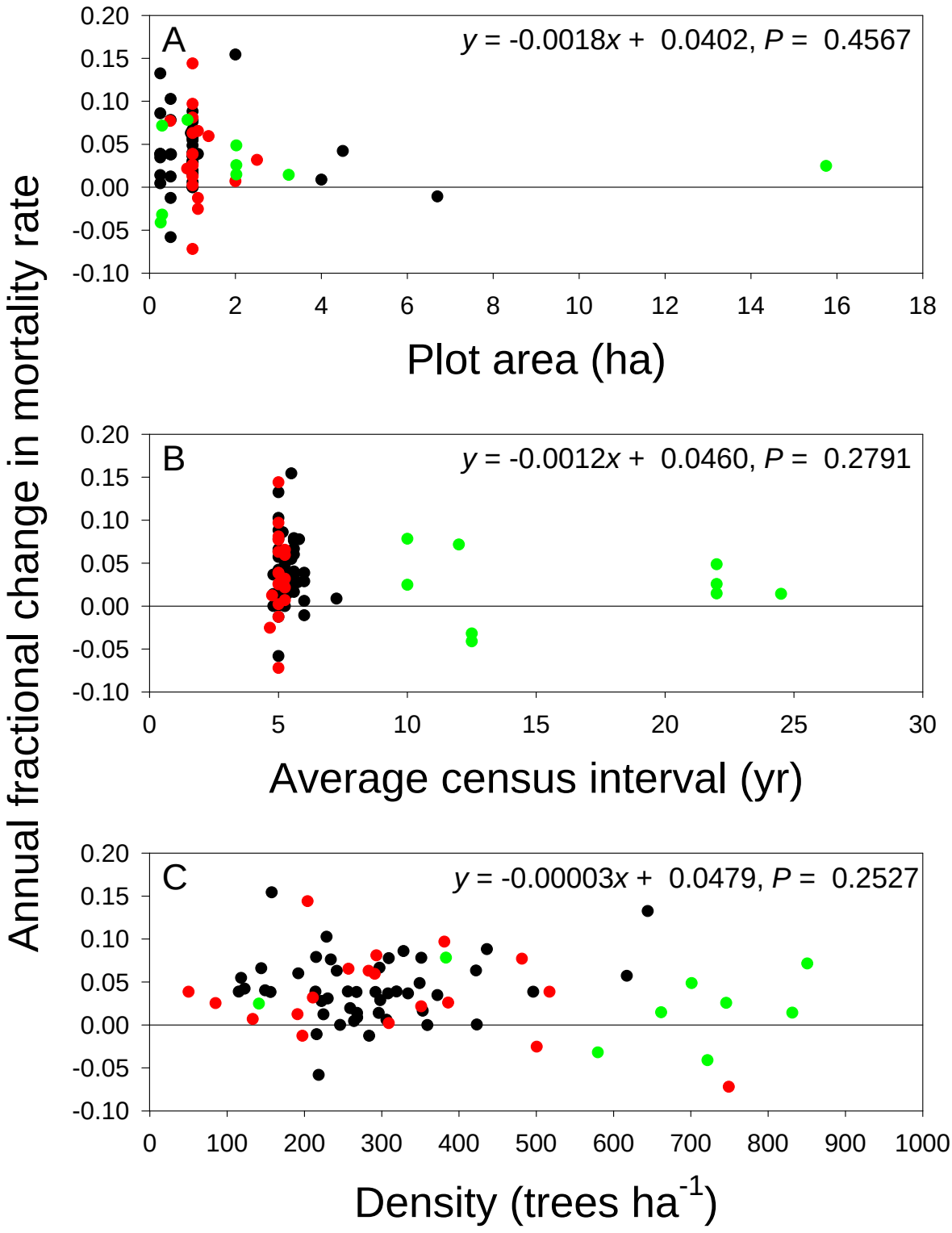

Figure S2. Modeled annual fractional change in mortality rate of individual plots relative to (A) plot area, (B) average census interval length, and (C) forest density. Black, red, and green symbols represent plots in the Pacific Northwest, California, and interior regions, respectively. Forest density was calculated as density of trees at the first census that were ≥15 cm in diameter, the minimum measured diameter common to all plots.

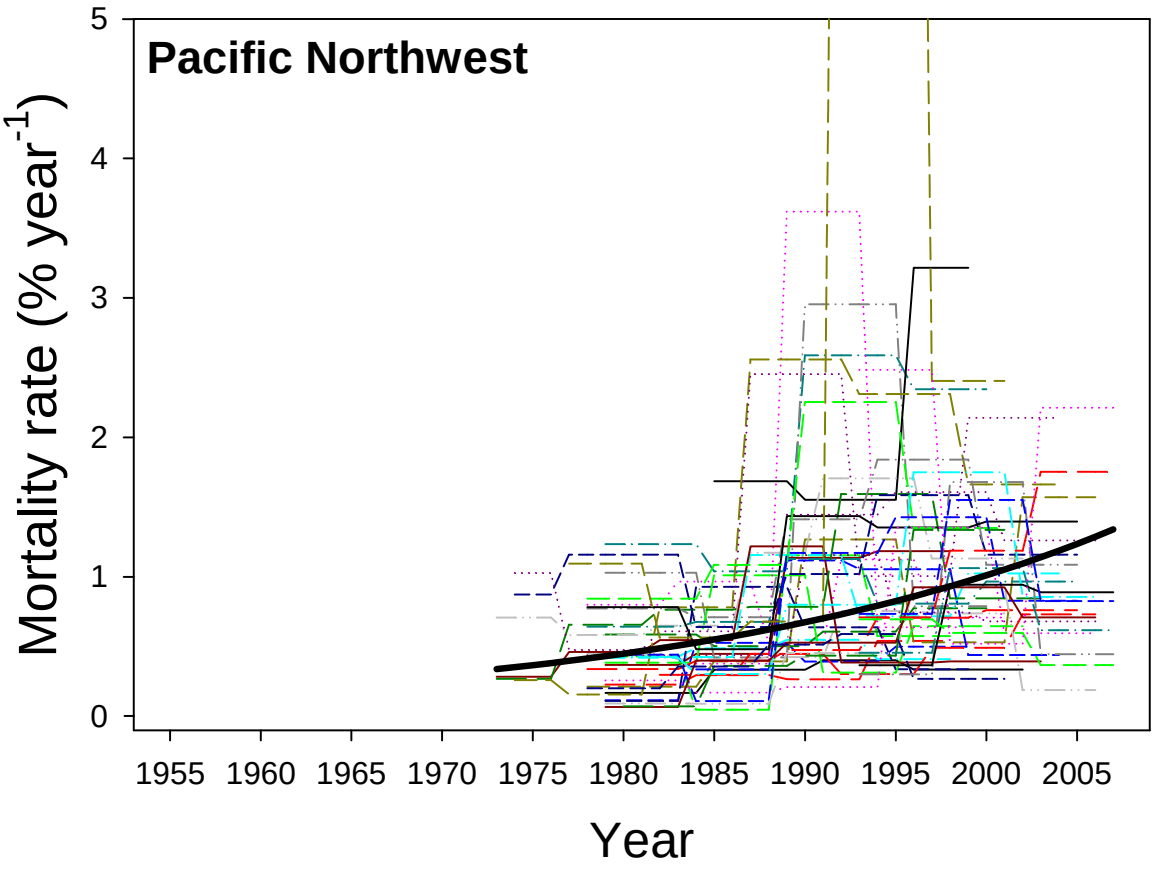

Figure S3. Mortality rate through time for each of the 47 plots in the Pacific Northwest region. Each horizontal line segment represents the mortality rate during a single census interval for a particular plot. The heavy black curve is the modeled trend in tree mortality rate for the Pacific Northwest region presented in Fig. 2A of the main article.

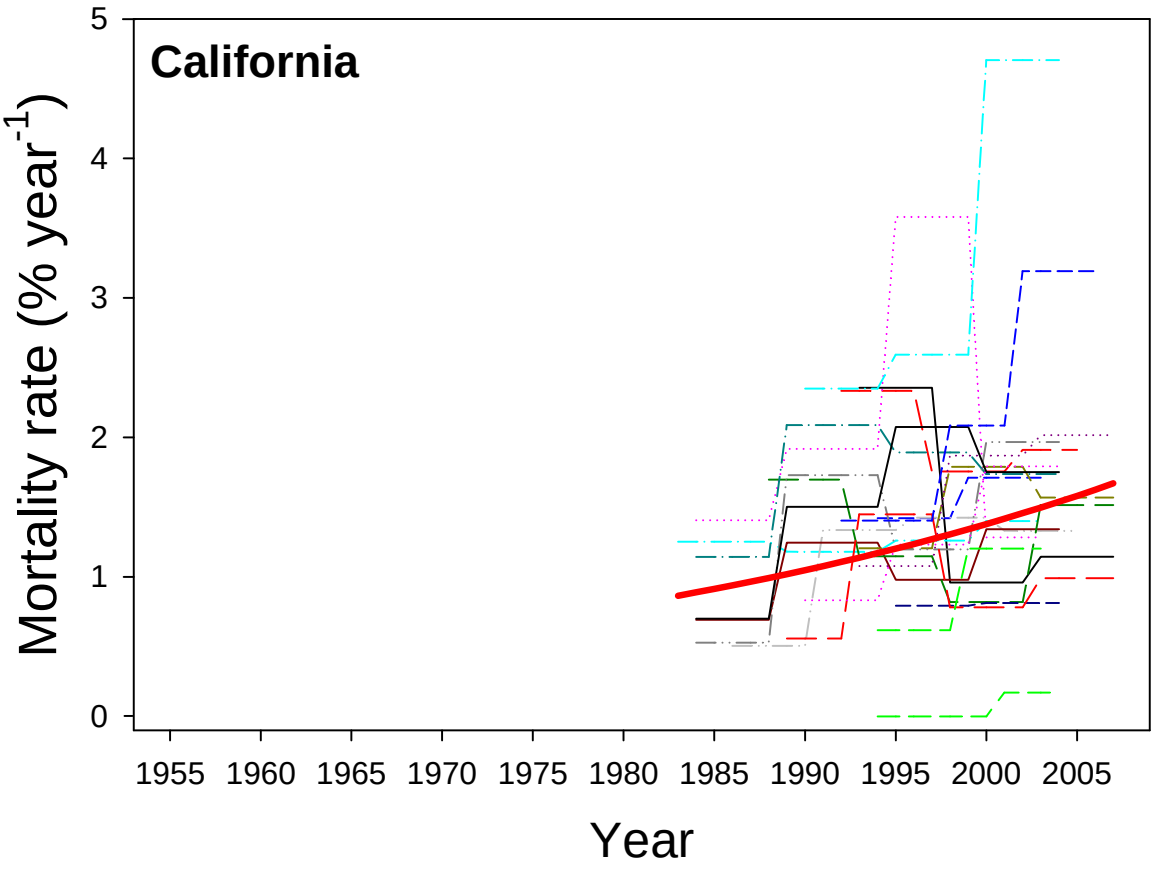

Figure S4. Mortality rate through time for each of the 20 plots in California. Each horizontal line segment represents the mortality rate during a single census interval for a particular plot. The heavy red curve is the modeled trend in tree mortality rate for the California region presented in Fig. 2A of the main article.

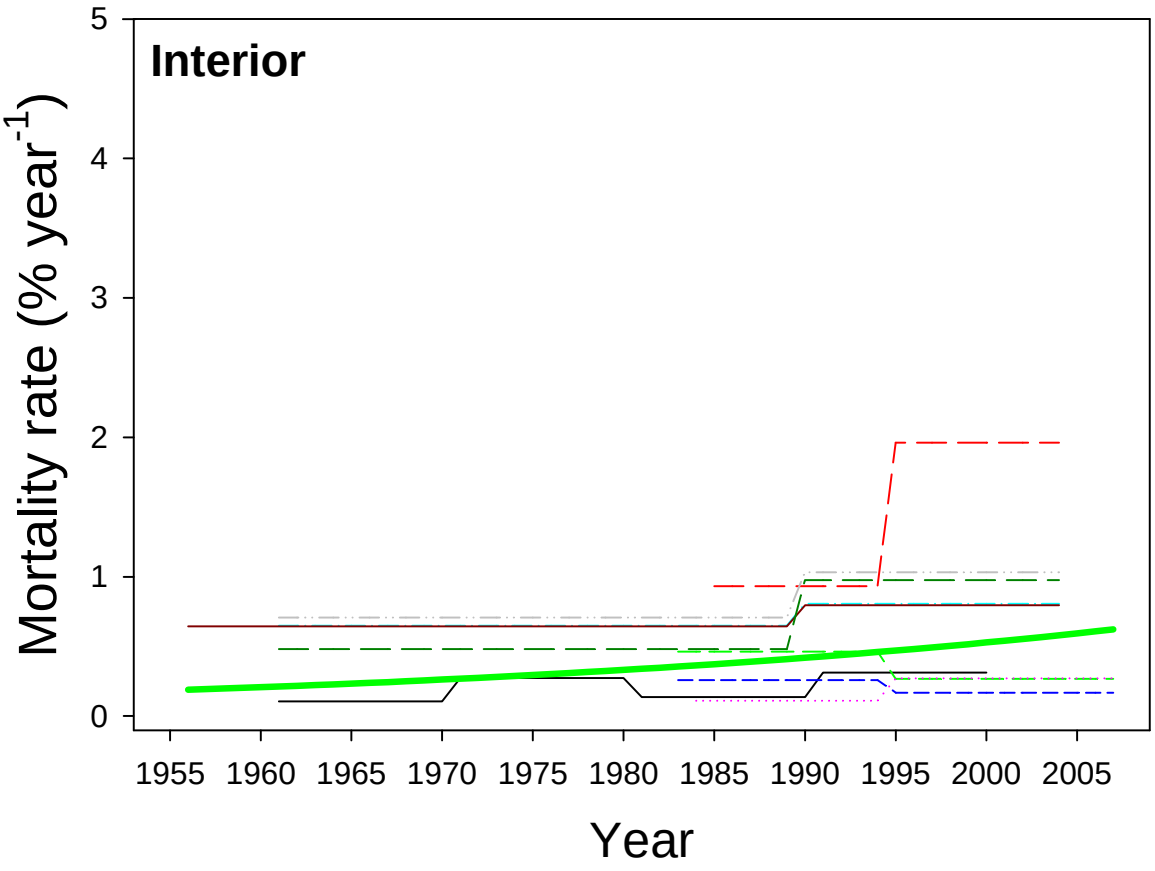

Figure S5. Mortality rate through time for each of the 9 plots in the interior region. Each horizontal line segment represents the mortality rate during a single census interval for a particular plot. The heavy green curve is the modeled trend in tree mortality rate for the interior region presented in Fig. 2A of the main article.

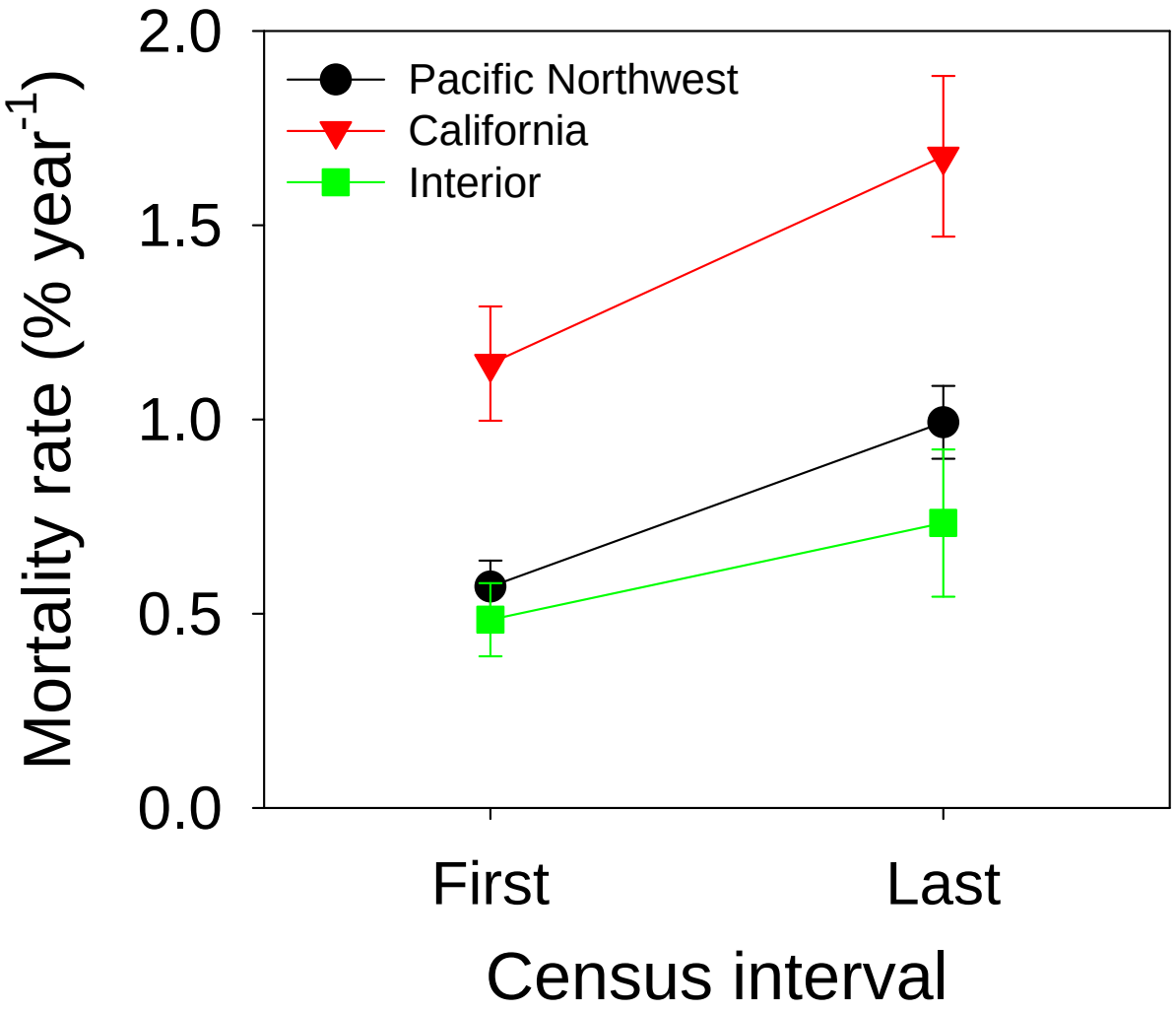

Figure S6. Mean mortality rates (±1 S.E.) for the first and last census intervals of all plots in each region. For each region, mean mortality rate of the last census interval is significantly higher than that of the first interval (Pacific Northwest, $P<0.0001$; California, $P<0.0001$; interior, $P=0.0078$, paired permutation tests). The calendar years of first and last census intervals, and the number of intervening years between the intervals, vary widely among plots (Table S1, Figs. S3-S5). Thus, the time periods spanned by the lines in this figure are shorter than those spanned by the modeled curves presented in Figs. S3-S5, which begin and end at the first and last censuses occurring in a particular region. Mean census interval midpoints for the first and last censuses in this figure are: Pacific Northwest, 1982-2000; California, 1991-2002; interior, 1979-1998.

Table S1. Characteristics of the 76 forest plots.

Plot identifier	Region*	Lat.°	Long.°	Fire Return Interval class†	Elevation (m)	Plot area (ha)	Minimum dbh (cm)	Live trees‡	Calendar year of censuses							Species comprising ≥ 1% of trees§
									year 1	year 2	year 3	year 4	year 5	year 6	year 7	
LDUN	1	49.5	-123.0	>250 (*S25*)	367	0.49	9.8	220	1992	1997	2002	2007				ABAM 49%, TSHE 44%, THPL7%
LD1A	1	49.5	-122.9	>250 (*S25*)	531	0.49	9.8	177	1992	1997	2002	2007				TSHE 70%, THPL 15%, ABAM 12%, TABR 3%
LD1B	1	49.5	-122.9	>250 (*S25*)	527	0.49	9.8	200	1992	1997	2002	2007				TSHE 75%, THPL 10%, TABR 6%, PSME 5%, ABAM 4%
LD1C	1	49.5	-122.9	>250 (*S25*)	538	0.49	9.8	220	1992	1997	2002	2007				TSHE 65%, THPL 19%, TABR 10%, ABAM 4%, PSME 1%
LDMA	1	49.5	-122.9	>250 (*S25*)	471	0.49	9.8	139	1992	1997	2002	2007				ABAM 45%, TSHE 37%, THPL 17%
LD2C	1	49.5	-122.9	>250 (*S25*)	425	0.49	9.8	175	1992	1997	2002	2007				TSHE 52%, ABAM 47%, THPL 1%
LD2B	1	49.5	-122.9	>250 (*S25*)	414	0.49	9.8	143	1992	1997	2002	2007				TSHE 79%, ABAM 16%, THPL 5%
HS04	1	47.8	-124.0	>250 (*S26*)	130	1.00	5.0	221	1984	1989	1995	1999				TSHE 53%, PISI 46%, PSME 1%
HR01	1	47.8	-123.9	>250 (*S26*)	215	1.00	5.0	167	1978	1984	1989	1995	2000			TSHE 52%, PISI 47%, PSME 1%, THPL 1%
HR02	1	47.8	-123.9	>250 (*S26*)	215	1.00	5.0	133	1978	1984	1989	1995	2000			TSHE 50%, PISI 48%, PSME 1%, THPL 1%
AV14	1	47.0	-121.8	>250 (*S26*)	1080	1.00	15.0	259	1978	1984	1990	1995	2000			ABAM 53%, TSHE 45%, CHNO 2%
AB08	1	46.9	-121.5	>250 (*S26*)	1050	1.00	15.0	298	1978	1984	1990	1995	2002			TSHE 71%, THPL 19%, PSME 6%, ABAM 2%, CHNO 1%
PP17	1	46.9	-121.6	25-250 (*S26*)	1120	1.00	15.0	306	1978	1984	1990	1995	2002			PSME 33%, PICO 29%, PIMO 14%, ABLA 8%, TSHE 6%, PIEN 5%, POTR2 3%, TSME 1%
AO03	1	46.8	-121.5	>250 (*S26*)	866	1.00	5.0	381	1977	1982	1987	1991	1996	2001		ABAM 72%, TSHE 25%, THPL 2%, PSME 1%
AV02	1	46.8	-121.6	>250 (*S26*)	850	1.00	5.0	1032	1977	1982	1987	1991	1996	2001		ABAM 83%, TSHE 16%, THPL 1%
CCNF	1	46.8	-121.8	>250 (*S26*)	1140	0.50	5.0	182	1978	1983	1989	1994	1999			TSHE 41%, ABAM 30%, ABPR 29%
AR07	1	46.8	-121.7	>250 (*S26*)	1430	1.00	15.0	423	1978	1983	1988	1993	1998			CHNO 37%, ABAM 35%, TSME 28%
AV06	1	46.8	-121.8	>250 (*S26*)	1060	1.00	15.0	436	1978	1983	1988	1993	1998			ABAM 63%, TSHE 33%, CHNO 1%, PSME 1%, THPL 1%
AM16	1	46.8	-121.8	>250 (*S26*)	1195	1.00	15.0	349	1978	1983	1989	1994	1999			ABAM 42%, CHNO 32%, TSME 19%, TSHE 7%
AE10	1	46.8	-121.7	>250 (*S26*)	1430	1.00	15.0	617	1978	1983	1988	1993	1998			CHNO 52%, ABAM 46%, ABLA 1%, TSME 1%
AG05	1	46.7	-121.8	>250 (*S26*)	950	1.00	15.0	422	1978	1983	1988	1993	1998			ABAM 47%, THPL 23%, TSHE 19%, PSME 5%, TABR 5%
TA01	1	46.7	-121.6	25-250 (*S26*)	670	1.00	5.0	399	1977	1982	1987	1991	1995	2001		TSHE 58%, PSME 35%, TABR 4%, ABAM 3%, THPL 1%
GMNF	1	46.2	-122.3	25-250 (*S26*)	945	4.00	15.0	1073	1977	1989	1994	1999	2006			ABAM 47%, TSHE 28%, ABPR 19%, PSME 6%
BRNA	1	44.9	-122.2	25-250 (*S26*)	650	1.00	5.0	405	1977	1984	1989	1995	2001	2006		TSHE 64%, PSME 31%, THPL 4%
RS25	1	44.5	-122.3	25-250 (*S27*)	457	1.13	5.0	434	1977	1984	1989	1995	2001			TSHE 81%, PSME 17%, CONU 2%
MRNA	1	44.5	-121.6	<25 (*S26*)	850	4.50	10.0	1420	1981	1986	1991	1996	2001	2006		PIPO 100%
SP06	1	44.4	-121.8	>250 (*S26*)	1464	0.25	5.0	224	1976	1981	1986	1991	1996	2001		TSME 95%, ABLA 4%, ABAM 1%
RS22	1	44.3	-122.1	25-250 (*S27*)	1290	1.00	5.0	651	1977	1983	1988	1993	1999	2005		ABAM 60%, ABPR 13%, TSHE 13%, TSME 10%, PSME 5%
RS04	1	44.3	-122.1	25-250 (*S27*)	1440	0.25	5.0	214	1972	1976	1981	1986	1990	1996	2002	ABAM 76%, PSME 20%, TSHE 3%, ABPR 1%

RS31	1	44.3	-122.2	25-250 (*S27*)	900	1.00	15.0	297	1978	1983	1988	1995	2001	2006		TSHE 75%, PSME 19%, THPL 3%, TABR 2%, ABAM 1%
RS03	1	44.3	-122.2	25-250 (*S27*)	950	1.00	5.0	474	1981	1986	1992	1998	2004			TSHE 57%, THPL 18%, TABR 10%, ABAM 8%, PSME 6%, CACH 1%
RS27	1	44.3	-122.2	25-250 (*S27*)	790	0.96	5.0	365	1978	1983	1988	1994	2000	2005		TSHE 46%, PSME 20%, TABR 19%, THPL 12%, ABAM 1%, ABGR 1%, CONU 1%
RS21	1	44.2	-122.1	25-250 (*S27*)	1190	1.00	5.0	615	1977	1983	1988	1993	1999	2005		ABAM 55%, TSHE 37%, PSME 7%
RS28	1	44.2	-122.2	25-250 (*S27*)	1060	1.00	15.0	234	1978	1983	1988	1994	2000	2006		TSHE 68%, PSME 21%, ABAM 6%, ABGR 3%, TABR 3%
RS10	1	44.2	-122.2	25-250 (*S27*)	610	0.25	5.0	187	1972	1976	1981	1986	1991	1997	2003	PSME 60%, TSHE 15%, CONU 11%, TABR 6%, THPL 4%, CACH 3%, ABGR 1%, PILA 1%
RS29	1	44.2	-122.1	>250 (*S27*)	800	1.00	15.0	192	1978	1983	1988	1995	2001	2006		TSHE 42%, THPL 32%, PSME 18%, TABR 8%, ABAM 1%
RS30	1	44.2	-122.1	25-250 (*S27*)	870	1.00	15.0	215	1978	1983	1988	1995	2001	2006		TSHE 49%, THPL 22%, PSME 21%, TABR 7%, ABAM 1%
RS23	1	44.2	-122.1	25-250 (*S27*)	1020	1.00	5.0	248	1977	1983	1988	1993	1999	2005		TSHE 50%, ABAM 16%, TABR 13%, PSME 10%, ABCO 5%, THPL 5%, PIMO 1%
RS20	1	44.2	-122.2	25-250 (*S27*)	700	1.00	5.0	527	1977	1983	1988	1993	1999	2005		PSME 89%, QUGA 4%, ARME 2%, ACMA 1%, CADE 1%, PILA 1%
RS17	1	44.2	-122.2	25-250 (*S27*)	500	0.25	5.0	131	1973	1976	1981	1986	1992	1998	2004	TABR 53%, TSHE 30%, PSME 11%, CONU 3%, THPL 2%, ACMA 1%
RS34	1	44.2	-122.2	25-250 (*S27*)	820	2.00	5.0	561	1979	1984	1989	1995	2001			TSHE 55%, THPL 25%, TABR 14%, PSME 6%, ABAM 1%, ACMA 1%
RS02	1	44.2	-122.2	25-250 (*S27*)	520	1.00	15.0	319	1983	1988	1993	1999				TSHE 71%, PSME 20%, TABR 5%, THPL 3%, CONU 2%
RS16	1	44.2	-122.2	25-250 (*S27*)	670	0.25	5.0	154	1973	1976	1983	1988	1993	1999	2005	CACH 48%, PSME 17%, TSHE 13%, CONU 10%, TABR 9%, PILA 1%, THPL 1%
RS15	1	44.2	-122.2	25-250 (*S27*)	720	0.25	5.0	129	1973	1976	1981	1986	1992	1998	2004	TSHE 54%, THPL 20%, ACMA 13%, PSME 9%, CONU 2%, TABR 2%
WS02	1	44.2	-122.2	25-250 (*S27*)	700	6.70	5.0	2628	1988	1994	2000	2006				TSHE 50%, PSME 21%, TABR 12%, CACH 6%, THPL 4%, ACMA 3%, CONU 3%
RS08	1	44.2	-122.3	25-250 (*S27*)	500	0.25	5.0	177	1972	1976	1981	1986	1991	1997	2003	PSME 75%, ACMA 11%, TABR 5%, CONU 4%, TSHE 2%, CACH 1%, CADE 1%
RS01	1	44.2	-122.3	25-250 (*S27*)	510	1.00	15.0	359	1983	1988	1992	1998	2004			PSME 88%, ACMA 7%, TABR 3%, ARME 1%, TSHE 1%
Swain Mt. 1	2	40.4	-121.1	<25 (*S10*)	1970	1.00	4.0	513	1989	1994	1999	2004				ABMA 88%, ABCO 12%
Swain Mt. 2	2	40.4	-121.1	<25 (*S10*)	1910	0.48	4.0	571	1989	1994	1999	2004				ABMA 78%, ABCO 22%
SFTRABMA	2	37.8	-119.7	25-250 (*S28*)	2484	1.00	0.1	1631	1992	1997	2002	2007				ABMA 100%
POFLABMA	2	37.8	-119.6	25-250 (*S28*)	2542	1.00	0.1	589	1994	1999	2004					ABMA 94%, PICO 6%
YOHOPIPO	2	37.8	-119.9	<25 (*S28*)	1500	1.00	0.1	2965	1991	1997	2001	2006				ABCO 35%, CADE 32%, PILA 26%, PIPO 5%, PSME 1%, QUKE 1%
CRCRPIPO	2	37.7	-119.8	<25 (*S28*)	1637	1.00	0.1	1753	1993	1998	2003					ABCO 44%, CADE 29%, PILA 18%, PIPO 6%, QUKE 2%
FRPIJE	2	36.6	-118.7	25-250 (*S28*)	2106	1.00	0.1	161	1983	1988	1994	1999	2003			PIJE 87%, ABCO 8%, CADE 2%, PILA 2%, PIMO 1% ¶
SUPILA	2	36.6	-118.8	<25 (*S28*)	2059	1.13	0.1	765	1983	1988	1994	1999	2004			ABCO 68%, PILA 21%, CADE 9%, QUKE 1%
SUABCO	2	36.6	-118.8	<25 (*S28*)	2035	0.88	0.1	680	1983	1988	1994	1999	2004			ABCO 59%, CADE 28%, PILA 9%, ABMA 4%
SURIP	2	36.6	-118.8	<25 (*S28*)	2033	1.38	0.1	1014	1983	1988	1994	1999	2004			ABCO 55%, CADE 20%, PILA 20%, ABMA 4%, QUKE 1%
WTABMA	2	36.6	-118.7	25-250 (*S28*)	2521	1.00	0.1	459	1993	1998	2003					ABMA 99%, PIMO 1%
PGABMA	2	36.6	-118.7	25-250 (*S28*)	2576	1.00	0.1	765	1992	1997	2002	2007				ABMA 100%
CCRPIPO	2	36.6	-118.8	<25 (*S28*)	1622	1.13	0.1	2101	1991	1996	2001	2005				ABCO 46%, CADE 30%, QUKE 15%, PILA 5%, PIPO 4%
LOGPIJE	2	36.6	-118.7	25-250 (*S28*)	2405	1.00	0.1	120	1985	1990	1995	2000	2005			ABCO 58%, PIJE 39%, ABMA 2%, PILA 1%
BBBPIPO	2	36.6	-118.8	<25 (*S28*)	1609	1.00	0.1	1273	1992	1997	2002	2007				CADE 55%, QUKE 24%, ABCO 12%, PILA 5%, PIPO 4%, QUCH 1%

LMCC	2	36.6	-118.7	<25 (*S28*)	2128	2.00	0.1	591	1982	1988	1994	1999	2003	ABCO 69%, ABMA 22%, SEGI 7%, PILA 2%
LOGSEGI	2	36.6	-118.7	<25 (*S28*)	2170	2.50	0.1	1055	1983	1988	1994	1999	2004	ABCO 76%, ABMA 15%, PILA 5%, SEGI 3%
UPLOG	2	36.6	-118.7	<25 (*S28*)	2210	1.00	0.1	407	1988	1992	1997	2002	2007	ABCO 89%, PILA 6%, CADE 2%, PIJE 1%, QUKE 1%
LOLOG	2	36.6	-118.7	<25 (*S28*)	2207	1.13	0.1	451	1987	1992	1997	2002	2007	ABCO 75%, ABMA 22%, PILA 2%, SEGI 1%
CIRQUE	2	36.5	-118.3	25-250 (*S28*)	3353	1.56	0.1	248	1993	2000	2004			PIBA 98%, PICO 2%
Priest River 148	3	48.2	-116.5	25-250 (*S29*)	2300	0.88	7.6	503	1984	1994	2004			TSHE 35%, ABGR 23%, THPL 23%, PIMO 12%, PSME 4%, LAOC 2%
MRS5	3	40.0	-105.6	>250 (*S30*)	3280	0.29	4.0	424	1982	1994	2007			ABLA 51%, PIEN 49%
MRS7	3	40.0	-105.6	>250 (*S30*)	3260	0.29	4.0	494	1983	1994	2007			ABLA 49%, PIEN 47%, PICO 2%, PIFL 2%
BW2	3	40.0	-105.6	>250 (*S30*)	2980	0.26	4.0	369	1982	1994	2007			PIFL 69%, ABLA 15%, PIEN 9%, PICO 5%, POTR 2%
FRB2	3	39.9	-105.9	>250 (*S30*)	2840	2.02	9.1	1509	1960	1989	2004			PICO 94%, PIEN 4%, ABLA 2%
FRC3	3	39.9	-105.9	>250 (*S30*)	2880	2.02	9.1	1986	1960	1989	2004			PICO 98%, ABLA 1%, PIEN 1%
FRD2	3	39.9	-105.9	>250 (*S30*)	2900	2.02	9.1	1875	1960	1989	2004			PICO 99%, ABLA 1%
FRD1	3	39.9	-105.9	>250 (*S30*)	2900	3.24	9.1	3528	1955	1989	2004			PICO 48%, PIEN 29%, ABLA 23%
Gus Pearson	3	35.3	-111.7	<25 (*S31*)	2255	15.75	8.9	3090	1960	1970	1980	1990	2000	PIPO 100%

* Numerals indicate groups of plots used in analyses by region: (1) Pacific Northwest, (2) California, and (3) interior.

† Fire return interval class (in years) was estimated from the cited sources (*S10, S25-31*).

‡ Count of live trees at the first census.

§ Species composition of trees at the first census. Percentages may not add to 100 due to rounding. ABAM = *Abies amabilis*, ABCO = *A. concolor*, ABGR = *A. grandis*, ABLA = *A. lasiocarpa*, ABMA = *A. magnifica*, ABPR = *A. procera*, ACMA = *Acer macrophyllum*, ARME = *Arbutus menziesii*, CACH = *Castanopsis chrysophylla*, CADE = *Calocedrus decurrens*, CHNO = *Chamaecyparis nootkatensis*, CONU = *Cornus nuttallii*, LAOC = *Larix occidentalis*, PIBA = *Pinus balfouriana*, PICO = *P. contorta*, PIEN = *Picea engelmannii*, PIFL = *Pinus flexilis*, PIJE = *P. jeffreyi*, PILA = *P. lambertiana*, PIMO = *P. monticola*, PIPO = *P. ponderosa*, PISI = *Picea sitchensis*, POTR = *Populus tremuloides*, POTR2 = *P. trichocarpa*, PSME = *Pseudotsuga menziesii*, QUCH = *Quercus chrysolepis*, QUGA = *Q. garryana*, QUKE = *Q. kelloggii*, SEGI = *Sequoiadendron giganteum*, TABR = *Taxus brevifolia*, THPL = *Thuja plicata*, TSHE = *Tsuga heterophylla*, TSME = *T. mertensiana*.

¶ *Q. kelloggii* (16 trees) was excluded from analysis at this plot due to inconsistent methods for censusing recruitment.

Table S2. Fixed effects of the generalized nonlinear mixed models describing recruitment rate trends. *a* is the annual fractional change in recruitment rate, *n* is the number of forest plots used in the model.

Model	Data	*a*	Std. Error	*P*	*n*
Recruitment trend	All plots	0.004	0.006	0.4359	61
Recruitment trend by region	Pacific Northwest	0.004	0.007	0.5898	40
	California	-0.002	0.011	0.8396	20
	Interior	-0.697	0.195	0.2041	1

Table S3. Fixed effects of generalized nonlinear mixed models investigating some possible causes of the widespread increase in mortality rates (see the main article). *a* is the estimated annual fractional change in mortality rate, *n* is the number of forest plots used in the model.

Possible cause	Data	*a*	Std. Error	*P*	*n*
Aging tree cohorts	Small tree standing dead*	0.043	0.007	<0.0001	53
Adding plots through time	Plots established by 1975	0.031	0.013	0.0333	11
	Plots established by 1980	0.043	0.006	<0.0001	39
	Plots established by 1985	0.040	0.005	<0.0001	55
	Plots established by 1990	0.040	0.005	<0.0001	60
Forest fragmentation	Inside national parks†	0.033	0.007	<0.0001	33
	Outside national parks	0.041	0.006	<0.0001	43

* Cause of death data for small trees (<15 cm dbh) were available for plots in the Pacific Northwest, California, and for the Gus Pearson plot (see table S1).

† Plots inside national parks were AB08, AE10, AG05, AM16, AO03, AR07, AV02, AV06, AV14, CCNF, HR01, HR02, HS04, PP17, TA01, BBBPIPO, CCRPIPO, CIRQUE, CRCRPIPO, FRPIJE, LMCC, LOGPIJE, LOGSEGI, LOLOG, PGABMA, POFLABMA, SFTRABMA, SUABCO, SUPILA, SURIP, UPLOG, WTABMA, and YOHOPIPO (see table S1).

Table S4. Fixed effects of the generalized nonlinear mixed models describing mortality rate trends with climate, where β represents estimated model parameters. There was little evidence for interactions between year and average temperature and between year and climatic water deficit.

Model	Parameter	β	Std. Error	P	n
Mortality trend with average temperature	Year	0.033	0.004	<0.0001	76
	Average annual temperature (^{o}C)	0.092	0.022	<0.0001	
Mortality trend with climatic water deficit	Year	0.033	0.005	<0.0001	76
	Average annual climatic water deficit (mm)	0.002	0.001	0.0066	

Supporting References and Notes

S1. P. Cherubini *et al.*, *Journal of Ecology* **90**, 839 (2002).
S2. S. A. Richards, E. A. Johnson., *Ecology* **88**, 1582 (2007).
S3. C. D. Oliver, B. C. Larson, *Forest Stand Dynamics*. (McGraw-Hill, Inc., New York, 1990), pp. 467.
S4. J. F. Franklin *et al.*, *Forest Ecology and Management* **155**, 399 (2002).
S5. P. Hall, P. S. Ashton, R. Condit, N. Manokaran, S. P. Hubbell, in *Forest Biodiversity Research, Monitoring, and Modeling: Conceptual Background and Old World Case Studies,* F. Dallmeier, J. A. Comisky, Eds. (UNESCO and Parthenon Publishing Group, Paris and New York, 1998), vol. 20, Man and the Biosphere Series, pp. 63-77.
S6. N. L. Stephenson, P. J. van Mantgem, *Ecology Letters* **8**, 524 (2005).
S7. W. B. Smith, *Environmental Pollution* **116**, S233 (2002).
S8. L. D. Daniels, *Forestry Chronicle* **79**, 517 (2003).
S9. S. A. Acker, W. A. McKee, M. E. Harmon, J. F. Franklin, in *Forest Biodiversity in North, Central and South America, and the Caribbean: Research and Monitoring,* F. Dallmeier, J. A. Comisky, Eds. (Man and the Biosphere Series, UNESCO and Parthenon Publishing Group, Paris and New York, 1998), vol. 21, pp. 93-106.
S10. A. H. Taylor, *Canadian Journal of Forest Research* **23**, 1672 (1993).
S11. P. J. van Mantgem, N. L. Stephenson, *Ecology Letters* **10**, 909 (2007).
S12. R. E. Alexander *et al.*, *Fraser Experimental Forest, Colorado: Research Program and Published Research 1937-1985*. (USDA Forest Service, Rocky Mountain Forest and Range Experimental Station, GTR-RM-118, Fort Collins, 1985), pp. 35.
S13. T. T. Veblen, *Bulletin of the Torrey Botanical Club* **113**, 225 (1986).
S14. C. C. Avery, F. R. Larson, G. H. Shubert, *Fifty-Year Records of Virgin Stand Development in Southwestern Ponderosa Pine*. (USDA Forest Service, Rocky Mountain Forest and Range Experimental Station, GTR-RM-22, Fort Collins, 1976), pp. 71.
S15. D. Sheil, R. M. May, *Journal of Ecology* **84**, 91 (1996).
S16. A. Das, J. J. Battles, P. van Mantgem, N. Stephenson, *Ecology* **89**, 1744 (2008).
S17. C. Daly, W. P. Gibson, G. H. Taylor, G. L. Johnson, P. Pasteris, *Climate Research* **22**, 99 (2002).
S18. Climatic data for the United States were taken from: http://www.ocs.orst.edu/prism/, last accessed February 21, 2008. Climatic projections covering the census years were not available for the seven plots in southwestern British Columbia. Monthly climatic records were therefore taken from the nearest complete weather station data at the Vancouver International Airport, 31 km distant from the average plot locations (data source: http://www.climate.weatheroffice.ec.gc.ca/climateData/canada_e.html, accessed February 20, 2008)
S19. C. J. Willmott, C. M. Rowe, Y. Mintz, *Journal of Climatology* **5**, 589 (1985).
S20. N. L. Stephenson, *American Naturalist* **135**, 649 (1990).
S21. S. L. Lewis *et al.*, *Journal of Ecology* **92**, 929 (2004).
S22. O. L. Phillips *et al.*, *Philosophical Transactions of the Royal Society of London B Biological Sciences* **359**, 381 (2004).
S23. W. F. Laurance, L. V. Ferreira, J. M. Rankin-de Merona, S. G. Laurance, *Ecology* **79**, 2032 (1998).
S24. J. D. Ray, "Gaseous Pollutant Monitoring Program, Annual Data Summary 2006" *Natural Resource Technical Report NPS ARD/NRPC/NRTR-2007/058* (National Park

Service, 2007). (URL: http://www.nature.nps.gov/air/Pubs/pdf/ads/2006/GPMP-XX.pdf).

S25. L. D. Daniels, R. W. Gray, *Journal of Ecosystems and Management* **7**, 44 (2006).

S26. J. K. Agee, *Fire Ecology of Pacific Northwest Forests*. (Island Press, Washington D.C., 1993).

S27. P. D. A. Teensma, *Fire history and fire regimes of the central western Cascades of Oregon.*, (Ph.D. dissertation, University of Oregon, Eugene, 1987).

S28. J. Fites-Kaufman, P. Rundel, N. Stephenson, D. A. Weixelman, in *Terrestrial Vegetation of California, 3rd ed,* M. Barbour, T. Keeler-Wolf, A. A. Schoenherr, Eds. (University of California Press, 2007), pp. 456-501.

S29. J. K. Smith, W. C. Fischer, *Fire ecology of the forest habitat types of northern Idaho*. (USDA Forest Service, Intermountain Research Station, INT-GTR-363, Ogden, 1997), pp. 142.

S30. J. S. Sibold, T. T. Veblen, M. E. González, *Journal of Biogeography* **32**, 631 (2006).

S31. J. H. Dieterich, *Chimney Spring Forest Fire History*. (USDA Forest Service, Rocky Mountain Forest and Range Experiment Station, Research Paper RM-220, Fort Collins, 1980), pp. 8.

S32. Any use of trade names is for descriptive purposes only and does not imply endorsement by the U.S. Government.